International Journal of Mass Spectrometry 198 (2000) 165–172

Cation pair formation from acetone following monochromatic soft x-ray absorption

Isao H. Suzuki*[a], Norio Saito[a]

Electrotechnical Laboratory, Umezono, Tsujuba, Ibaraki 305-8568, Japan

Received 8 November 1999; accepted 12 January 2000

Abstract

Formation of positive ion pairs from acetone photoexcited into inner-shell hole states has been studied using monochromatized synchrotron radiation and a photoion–photoion coincidence technique. Significant effect of site-selective reaction on pathways for ion-pair formation has not been found near the C K-edges and the O K-edge. Ion-pair groups of H^+–CH_m^+ ($m = 0$–3) show the highest yield, and groups of H^+–$C_2H_m^+$ and H^+–$C_3H_m^+$ have considerable yields. In comparison with the single ion detection, ion pairs containing smaller number of hydrogen atoms are usually produced with higher yields than those with larger number of hydrogens. (Int J Mass Spectrom 198 (2000) 165–172) © 2000 Elsevier Science B.V.

Keywords: Cation pair formation; Inner-shell excitation; Photoion–photoion coincidence; Yield ratios; Acetone

1. Introduction

Excitation and ionization of a core electron in a molecule is usually accompanied by an Auger type decay, which often yields a doubly charged molecular ion. This molecular ion mostly decomposes into two ionic fragments and neutral species. The position of the bond breaking is possibly affected by the state or internal energy of the molecular ion, which is generated through the Auger transition. The orbital having a large overlap with the created core hole participates in this transition more frequently than the orbital far away from the core hole. Therefore the core electron excitation is expected to provide a particular fragmentation pattern strongly dependent on the site of the core hole. This site selectivity has been demonstrated by the yield spectra of some fragment ions from several molecules [1–8]. In the instance of the formation of a positive ion pair, a significant variation in the yield of a few ion pairs has been found in the inner-shell ionization regions. Some fragment ions produced from acetone, $(CH_3)_2CO$, near the C K-edges were reported to show a clear site selectivity in a single ion detection [9]. However this effect has not been confirmed with the measurement near the O K-edge [10] and with a precise re-measurement near both the C K-edges and the O K-edge by the present authors [11]. The difference among those studies possibly comes from different measurement techniques. The latter two studies utilized time-of-flight (TOF) mass spectrometers, whereas the former used a quadrupole mass spectrometer. The TOF spectrometer is often utilized for studies on ionic fragmentation of molecules following photoexcitation of inner-shell electrons in these years. The photon resolution in the former study seemed to be low, judging from the ion yield spectra [9]. On the other hand, there has been no work on the

---

*Corresponding author. E-mail: isuzuki@etl.go.jp

PII S1387-3806(00)00186-X

measurement of cation pair formation from acetone ionized with synchrotron radiation. These ion pair processes are usually studied using a photoion–photoion coincidence (PIPICO) technique, which enables us to detect two positive ions produced just from the identical molecular ion. This technique often observes fragmentation pathways much different from those identified with the single ion detection (non-coincidence). Since inner-shell ionization usually produces two or more fragment ions from a molecule, the PIPICO technique is a powerful tool for studies of ionic fragmentation in the soft x-ray region. Excitation of an electron from a core to a vacant orbital yields a molecular ion in a singly charged excited state, which turns into a fragment ion and neutrals sometimes and/or becomes two fragment ions and a neutral in other instances. Some groups provided nice outcomes on fragmentation pathways from inner-shell excited states of small molecules [12–15].

Ionic fragmentation and photoelectron spectra of acetone were studied using an electron beam and vacuum ultraviolet radiation [16–20]. Inner-shell excitation spectra were observed using monochromatized synchrotron radiation and an electron energy loss technique [21,22]. Excitation into the π* orbital was found as clear peaks in the regions of the C *K*-edges (291.1 and 293.7 eV) and the O *K*-edge (537.9 eV). The transition of methyl's C 1*s* electron to Rydberg orbitals was observed as a wider peak in the C *K*-edges region.

It is interesting to measure ion-pair formation from acetone photoexcited to inner-shell excited states because this molecule has three atomic sites of different chemical environments and because there is no study on ion-pair processes. In the present study pairs of positive fragment ions have been detected using a TOF mass spectrometer operated in a mode of PIPICO. Yield spectra for these ion pairs were observed in detail in the regions of the C *K*-edges and the O *K*-edge. Ratios for ion-pair yields were estimated at several photon energies.

2. Experimental

In order to obtain monochromatic soft x rays from 280 to 570 eV, synchrotron radiation from the TERAS electron storage ring at the Electrotechnical Laboratory was dispersed using a Grasshopper monochromator [4–8]. By selecting appropriate energies for the electron beam in the storage ring, the spectral distribution of the synchrotron radiation was modified to reduce the intensity of higher energy photons in the "white" light and thereby minimize higher order contributions to the monochromatized beam. Thin films of Al and In were also used as filters to reduce the scattered light and higher order contributions. A new grating of 2400 L/mm was installed into the monochromator, yielding about 5 times higher intensity near the C *K*-edges than that of the old grating. This result confirms that the intensity variation of the photon beam has significantly decreased at these edges, which is expected to provide reliable experimental data even at the C *K*-edges. Monochromatized synchrotron radiation (resolution, $E/\Delta E$,: about 250 at the C *K*-edges and intensity: about 2×10^8 photons/s) entered an experimental chamber equipped with a TOF mass spectrometer. The photon beam crossed an effusive beam of the sample gas at the center of the spectrometer, and the electrons and ions produced were extracted in opposite directions and detected with micro-channel plates. The axis of the TOF spectrometer was set at 55° to the photon polarization direction for reducing anisotropic effect in the photoabsorption process. Flight times of the photoions were monitored using a time-to-amplitude converter combined with a pulse-height analyzer. The electric field applied at this center was set to be 133 V/mm in order to collect ions of all kinetic energies. In order to obtain signals for ion-pair formation, ion signals were supplied to the start and the stop connectors in the time-to-amplitude converter (conventional PIPICO technique) [7,8]. The mass resolution, $m/\Delta m$, was about 45, as seen in Figs. 1 and 3.

3. Results and discussion

3.1. C K-edges region

Ion pairs produced from acetone have been measured by using the photoion–photoion coincidence

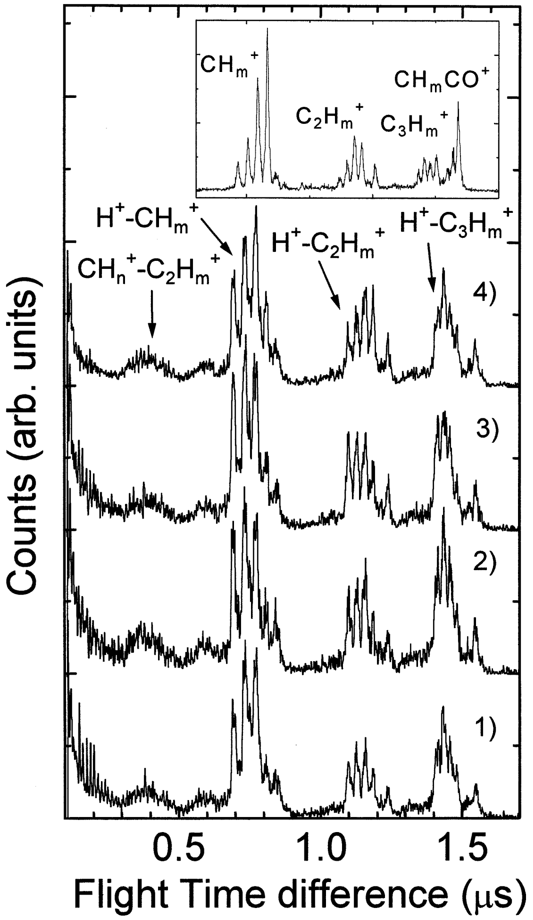

Fig. 1. Spectra of the difference in flight times between fragment ions from acetone at several photon energies near the C *K*-edges. (1) Below the C 1*s* electron excitation (285 eV). (2) Excitation of the carbonyl's C 1*s* electron into the π^* orbital (286.8 eV). (3) Excitation of the methyl's C 1*s* electron into Rydberg orbitals (288.4 eV). (4) Above the C 1*s* electron ionization thresholds (302 eV). The inset shows the TOF spectrum of fragment ions (non-coincidence) at the C 1*s* electron into the π^* orbital excitation (286.8 eV). The subscript *m* ranges from 0 to 3 for most ions. In the instance of $C_2H_m^+$, *m* mainly denotes 0–3 and 5. Ions of $m/z = 16$ and 28 are primarily O^+ and CO^+, respectively.

technique (PIPICO). Fig. 1 shows several PIPICO spectra observed in the region of C 1*s* transitions. Most of peaks or structures correspond to signals of ion pairs composed of H^+ and other fragment ions. Assignment for ion-pair group is shown in Fig. 1. Structures around 0.4 μs exhibit signals for ion-pair groups of CH_n^+ and $C_2H_m^+$ $(n, m = 0\text{–}3)$. The spectra at the bottom were measured at a photon energy (285 eV) below the C 1*s* excitation. Other spectra were obtained at 286.8 eV (the carbonyl's C 1*s* to π^* orbital), 288.4 eV (the methyl's C 1*s* to Rydberg orbitals), and 302 eV (above the C 1*s* ionization thresholds), from the lower to the upper, respectively. The inset at the top exhibits the TOF spectrum of fragment ions observed at 286.8 eV. The most intense signals come from the ion-pair group of H^+–CH_m^+ in the all spectra of Fig. 1, in particular the ion pairs of H^+–CH^+ and H^+–CH_2^+ are the highest two. The ion-pair group of H^+–$C_3H_m^+$ shows significant intensities and the H^+–$C_2H_m^+$ group exhibit relatively high peaks. The ion pair of H^+–C_3H^+ has the fourth highest yield in this energy region. Some signals below 0.3 μs are supposed to include considerable noises originating from interference of pulse processing [23]. The non-analyzed signals below 0.3 μs are presumed to be H^+–H^+ mainly, which possibly has a yield ratio of several percent, from consideration of the yield ratio with the non-coincidence detection [11].

In comparing individual peak heights within each ion-pair group, the ion pairs composed of the fragment ions containing a small number of hydrogen atoms show high yields, in particular in the instance of the Rydberg excitation. This finding in the ion-pair group with one carbon atom gives a clear contrast to the result by the single ion measurement (non-coincidence); The fragment ion including three hydrogen atoms, CH_3^+, showed the highest yield within the fragment ion group of one carbon atom [11]. (See the inset of Fig. 1, which exhibits the TOF spectrum with the non-coincidence of acetone at 286.8 eV.) This fact suggests that the following processes take place frequently.

$$(\text{acetone})^{2+} \longrightarrow CH_3^+ + F_1^+ + F_2 \qquad (1a)$$

$$\phantom{(\text{acetone})^{2+}} \longrightarrow CH^+ + H^+ + F_3 + H \qquad (1b)$$

In Eq. (1), F_1, F_2, and F_3 denote some fragments. The doubly charged molecular ion is formed through an Auger type decay via the initial inner-shell excitation.

Table 1.
Yield ratios for individual ion pairs at several photon energies (in units of %)[a]

	Photon energy (eV)						
Ion pair	285	287	288	302	526	531	545
H–C	9.2	8.4	9.7	7.8	14.0	11.8	12.0
H–CH	13.6	10.8	11.5	10.0	11.6	10.3	11.6
H–CH_2	17.7	11.8	13.4	14.1	11.9	10.5	12.6
H–CH_3	3.9	4.1	4.5	5.7	4.5	4.1	4.7
H–O	4.0	3.3	3.1	3.1	5.6	5.0	5.8
H–C_2	3.1	3.8	4.5	3.6	5.5	4.8	4.5
H–C_2H	2.2	4.4	4.7	4.8	5.0	4.5	4.4
H–C_2H_2	4.3	5.5	5.0	6.0	4.5	4.7	4.7
HC–C_2H_3	3.1	2.2	2.6	4.0	2.4	2.1	2.7
H–CH_2CH_3	1.6	2.0	1.9	2.4	1.8	1.5	1.6
H–C_3	5.6	5.9	6.2	5.2	5.5	5.7	5.3
H–C_3H	6.5	7.1	7.4	6.9	6.8	7.5	7.3
H–C_3H_2	5.5	5.5	4.2	4.5	3.0	4.1	3.2
H–C_3H_3	3.6	3.1	2.3	2.9	1.6	2.6	1.6
H–CH_mCO	1.5	3.8	3.3	3.8	2.5	2.9	2.5
CH_n–C_2H_m	9.6	11.4	9.9	9.5	7.7	10.2	8.7
Others	6.7	7.3	6.4	5.9	5.6	7.2	6.0

[a] N.B.: signals at a smaller flight time difference less than 300 ns are omitted because those can not be estimated correctly.

In process (1a), the charge distribution of the parent ion is supposed to be relatively expanded in the whole molecule, while the charge is probably localized in a particular methyl group in process (1b). The counterpart ion of CH_3^+ is not H^+ in many cases, but corresponds to several types of ions, whose signals are distributed in a wide range of the PIPICO spectra. These considerations can explain the difference in yields of CH_3^+ between the PIPICO measurement and the single ion measurement. The sample labeled with deuteron (D) is supposed to serve to clarify this statement and then deuterated acetone is being studied in the near future.

Another prominent feature is low intensity of H^+–CH_mCO^+ in all the PIPICO spectra. The fragment ion group of CH_mCO^+ showed considerable yields in the non-coincidence detection below the C 1*s* ionization threshold [11]. The present finding supports the previous work that most of this ion group are formed through dissociation of singly charged molecular ions.

Yield ratios for individual ion pairs have been estimated from areas in the PIPICO spectra. Table 1 lists the yield ratios for ion pairs at typical photon energies in the C *K* and O *K* regions. Some rows near the bottom denote the sum of the yield ratios for the ion-pair groups of H^+–CH_mCO^+ and CH_n^+–$C_2H_m^+$ and those for all other ion pairs. These lists were written because yields for individual ion pairs are difficult to be estimated accurately. Dramatic change in the yield ratios has not been found although the ratios vary slightly owing to initial excited states. Below the C 1*s* electron excitation, ion pairs are produced through two valence electron ionization by photon impact as follows

$$\begin{aligned} \text{acetone} + h\,\nu \rightarrow\ & \text{acetone}^{2+}(v^{-2}) + 2\text{e} \\ & \hookrightarrow F_1^+ + F_2^+ + F_3 \qquad (2) \end{aligned}$$

In this scheme, v denotes a valence orbital and F_m ($m = 1$–3) indicates a fragment. Although a probability of the two valence electron ionizations is usually low, as shown in Fig. 2, appreciable quantity of doubly charged ions are formed below the inner-shell excitation energy in the instance of rare gas atoms [24]. Ratio of double ionization seems to depend on the number of valence electrons. Acetone molecule has 12 valence orbitals and then it is not

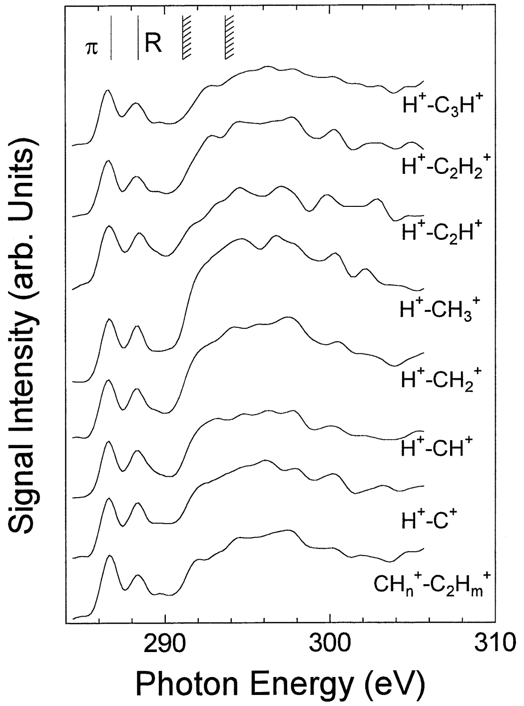

Fig. 2. Yield spectra for several ion pairs produced from acetone in the C 1*s* transition region. The bars denote the energy positions for the C 1*s* (of CO) to the π^* orbital excitation, the C 1*s* (of CH_3) to Rydberg orbital excitation, the C 1*s* (of CH_3) ionization threshold, and the C 1*s* (of CO) ionization threshold, from lower energy to higher, respectively.

surprising that double valence ionization takes place with relatively high probability.

Signal intensities for individual ion pairs have been measured as a function of photon energy (see Fig. 2). The bars in Fig. 2 denote the energy positions for transitions into the π^* orbital, Rydberg orbitals, the methyl's C 1*s* ionization (291.1 eV) and the carbonyl's C 1*s* ionization (293.7 eV) [21,22]. All yield spectra shown have a feature similar to one another, which exhibit peaks at the resonance excitation and increases near the ionization thresholds. Yield spectra of fragment ions in the single ion detection (noncoincidence) have a feature similar to photoabsorption spectra (or electron energy loss spectrum) [21,22]. In comparison with the instance of the single ion detection, PIPICO yields are higher above the ionization thresholds than the resonance excitation. This finding probably comes from the following. After the C 1*s* ionization, an Auger transition usually takes place and the molecule turns into a doubly charged ion. This ion decomposes to two fragment ions and other neutral species, as follows

$$\begin{array}{l} \text{acetone}^{+}(\text{C } 1s^{-1}) \rightarrow \text{acetone}^{2+}(v^{-2}) + e \\ \qquad\qquad\qquad\qquad\qquad \hookrightarrow \text{F}_1^{+} + \text{F}_2^{+} + \text{F}_3 \end{array} \tag{3}$$

However, different charge states are mainly responsible for fragmentation in the instance of the resonance excitation. The core-excited neutral state emits an electron in many cases although a considerable portion of the decay process is to eject two electrons simultaneously or successively [25]

$$\text{acetone}^{*}(\text{C } 1s^{-1}\text{Re}) \rightarrow \text{acetone}^{+}(v^{-1}) + \text{e} \tag{4a}$$

$$\rightarrow \text{acetone}^{+}(v^{-2}\text{Re}) + \text{e} \tag{4b}$$

$$\rightarrow \text{acetone}^{2+}(v^{-2}) + 2\text{e} \tag{4c}$$

In these schemes, Re denotes the π^* or Rydberg orbitals. Deexcitation (4a) indicates the participator Auger transition, in which the excited electron takes part in this transition, while the spectator decay happens in deexcitation (4b), in which the excited electron does not participate in the decay. The latter process occasionally emits another electron because the formed singly charged ion exists in relatively high excited states. Since an ion pair can be produced via a doubly charged state, the resonance excitation provides ion pairs at smaller yields than the inner-shell ionization [26,27].

In comparing the two kinds of the resonance excitation, the π^* excitation is usually involved in the participator decay because of high probability in overlapping of related wave functions. The Rydberg excitation is connected with the spectator decay with a high probability owing to low overlapping of the wave functions [25–27]. This phenomenon is supposed to induce higher ion-pair yields in the Rydberg excitation than those at the π^* excitation. The peak heights for the π^* excitation seem larger than those for the Rydberg excitation in Fig. 2. However, the peaks for the Rydberg transition become higher in the PIPICO yields (Fig. 2) in a relative scale than those in the instance of the single ion detection (the previous work) [11].

The characteristic profile of the yield spectrum is provided by the ion pair of H^+–CH_3^+, which exhibits a considerably higher intensity above the ionization thresholds than that at the resonance excitation. The ion pair of H^+–CH_2^+ shows a similar feature. These findings are probably connected to the result in the single ion detection. The yield ratios for CH_2^+ and CH_3^+ become high through the C 1*s* ionization.

Yield spectra for H^+–C^+, H^+–C_2H^+, and H^+–C_3H^+ exhibit a high peak at the Rydberg excitation. Those for other ion pairs have a lower peak at this energy than that at the π^* excitation. This finding is possibly related to the increase in the yield ratios of these fragment ions in the single ion measurement. The Rydberg excitation induces C–H bond rupture frequently, generating intensity increases in the fragment ions containing smaller number of hydrogen atoms. As Table 1 shows the difference in the yield ratios, fragment ions containing larger number of hydrogen atoms have lower yield ratios at the Rydberg excitation than the π^* excitation.

3.2. O K-edge region

Spectra of flight time differences have been measured at typical photon energies, 526 eV (below the O 1*s* excitation), 531.3 eV (the O 1*s* into the π^* orbital excitation), and 545 eV (above the O 1*s* ionization threshold) [21]. Fig. 3 shows these spectra from the bottom to the top, respectively. The spectra exhibit a similar feature to those in the C K-edge region. However, ion pairs composed of H^+ and fragment ions containing smaller number of hydrogen atoms show higher peaks than those in the C *K*-edge region. In particular H^+–C^+ and H^+–C_2^+ have higher yields below and at the resonance excitation than other ion pairs within each ion-pair group (H^+–CH_m^+ and H^+–$C_2H_m^+$). In the group of H^+–$C_3H_m^+$, H^+–C_3^+ shows the second highest peak, considerably higher than that of H^+–$C_3H_2^+$, although the highest peak is yielded by H^+–C_3H^+. These findings seem similar to the spectra observed at the excitation of the C 1*s* electron into Rydberg orbitals. The latter excitation induces the rupture of C–H bonds, forming the fragment ions containing fewer hydrogen atoms.

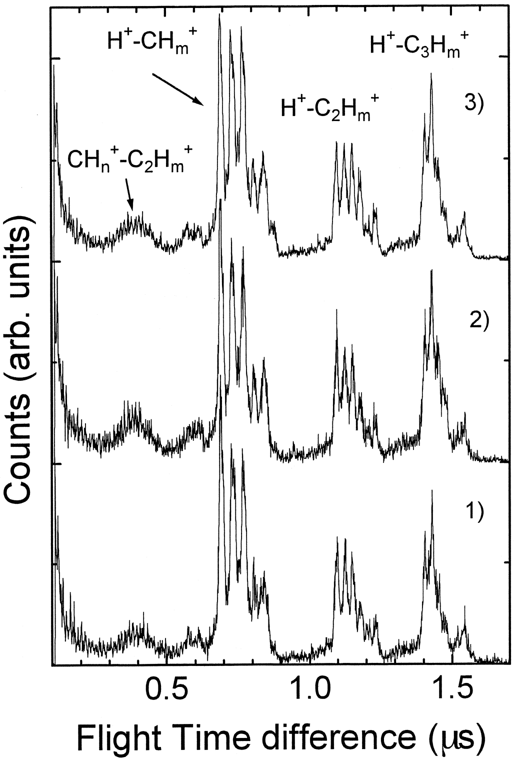

Fig. 3. Spectra of the difference in flight times between fragment ions from acetone at some photon energies near the O *K*-edge. (1) Below the O 1*s* electron excitation (526 eV). (2) Excitation of the O 1*s* electron into the π^* orbital (531.3 eV). (3) Above the O 1*s* electron ionization threshold (545 eV). The subscript *m* ranges from 0 to 3 for most ions. In the instance of $C_2H_m^+$, *m* mainly denotes 0–3 and 5. Ions of $m/z = 16$ and 28 are primarily O^+ and CO^+, respectively.

At the excitation of 526 eV, the spectrum of the flight time difference slightly differ from that at 302 eV (above the C *K*-edges). At 302 eV, photoionization of the C 1*s* electrons mainly happens, and then doubly charged ion states are formed through the normal C 1*s* Auger decay. The slight difference in the spectra between 526 and 302 eV suggests that another phenomenon takes place at 526 eV. One of most probable processes is the photoionization shake-off of the C 1*s* electron, which induces ionization or excitation of a valence electron [24]. One example of this process is expressed with the following

$$\begin{aligned} &\text{acetone} + h\nu \rightarrow \text{acetone}^{+2}(\text{C } 1s^{-1}v^{-1}) + 2e \\ &\qquad \hookrightarrow \text{acetone}^{+3}(v^{-3}) + e \\ &\qquad\qquad \hookrightarrow \text{H}^{+} + \text{C}^{+} + \text{F}_4^{+} + \text{F}_5 \end{aligned} \tag{5}$$

In process (5), F_4 and F_5 denote a certain fragment.

At the π^* orbital excitation, the PIPICO spectrum is similar to that at 526 eV. However, the molecular ion states formed through Auger type decays via the O $1s^{-1}$ π^* state are mainly singly charged ones. Then different pathways are considered to contribute to formation of ion pairs. Spectator Auger transitions occasionally yield highly excited ionic states, and then the formed ions emit another electron. The doubly charged ions finally formed have a possibility for holding vacancy in valence orbitals with C–H bonding character. Because of loosened C–H bonds, the molecular ions turn into the fragment ion containing smaller number of hydrogen atoms and other species with an appreciable rate [7,8]. This possibility seems to be realized in the middle of Fig. 3, in which ion pairs of H^+–C^+ and H^+–C_2^+ have high yields.

Fig. 4 shows the yield spectra of PIPICO signals in the O *K*-edge region. The bars denote the energy positions of the π^* resonance (531.5 eV) and the ionization threshold (537.9 eV) [21]. The most interesting point is a peak at the π^* resonance in the spectrum of H^+–$C_3H_3^+$. The spectra for H^+–C_3H^+ and CH_n^+–$C_2H_m^+$ (n, m = 0–3) show a similar feature to that of H^+–$C_3H_3^+$. Other ion pairs seem to have intensity increases, but the yields are lower than those above the ionization threshold. In the single ion measurement, the fragment ion of $C_3H_3^+$ exhibits a sharp peak at this energy. This resonance phenomenon indicates the existence of the site-selective fragmentation; the O 1*s* to π^* orbital excitation selectively increases the formation of the ion pair of H^+–$C_3H_3^+$. However it is noted that this ion pair is not a major product but has a small yield ratio.

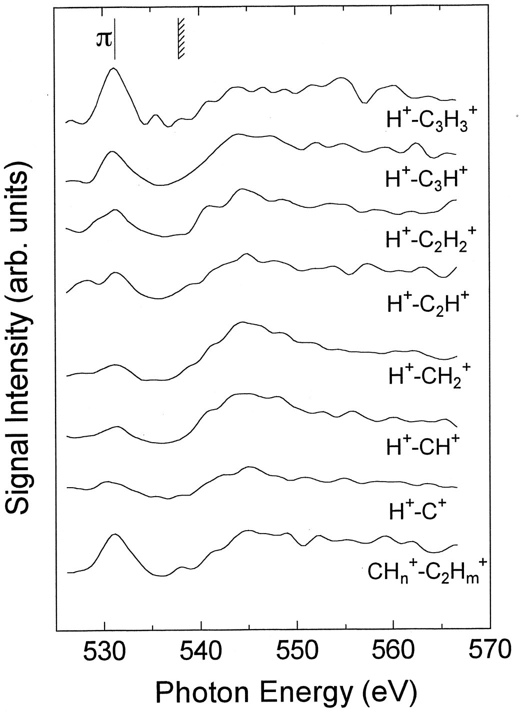

Fig. 4. Yield spectra for several ion pairs produced from acetone in the O 1*s* transition region. The bars denote the energy positions for the O 1*s* to the π^* orbital excitation and the O 1*s* ionization threshold.

Other ion pairs have considerably higher yields above the threshold than the π^* resonance although the spectra seem to have a similar feature to the electron energy loss spectrum [21]. This finding is reasonable because main decay processes at the π^* resonance yield singly charged ions, but do not form ion pairs. Ion pairs whose yield spectra are not shown in Fig. 4 have similar characteristics to those of H^+–$C_2H_2^+$ and H^+–CH_2^+.

4. Summary

The formation of ion pairs from acetone following monochromatic soft x-ray absorption has been studied by using the photoion–photoion coincidence technique. The ion-pair group of H^+–CH_m^+ ($m = 0$–3) has shown the highest yield in the C 1*s* and the O 1*s* electron transition regions. The ion pair group of H^+–$C_2H_m^+$ and H^+–$C_3H_m^+$ had considerable yields, and those for other ion pairs were not high. In comparison with the results of the single ion detection, ion pairs consisting of the fragment ions containing smaller number of hydrogen atoms showed higher yields than those with more hydrogen atoms. In particular H^+–C^+ and H^+–C_2^+ exhibited high yields at the excitation of the C 1*s* into Rydberg orbitals. The resonance excitation to the O $1s^{-1}$ π^* state induced selective formation of the ion pair of H^+–$C_3H_3^+$.

Acknowledgements

The authors with to express their sincere thanks to the staff of the accelerator group at ETL for their continued operation of TERAS electron storage ring.

References

[1] D.M. Hanson, Adv. Chem. Phys. 77 (1990) 1.
[2] I. Nenner, J.A. Beswick, In G.V. Marr (Ed.), Handbook on Synchrotron Radiation, North-Holland, Amsterdam, 1987, Vol. 2, p. 355.
[3] S. Nagaoka, J. Oshita, M. Ishikawa, T. Masuoka, I. Koyano, J. Phys. Chem. 97 (1993) 1488.
[4] I.H. Suzuki, J.D. Bozek, N. Saito, Chem. Phys. 182 (1994) 81.
[5] I.H. Suzuki, N. Saito, J.D. Bozek, Bull. Chem. Soc. Jpn. 68 (1995) 1119.
[6] N. Saito, J.D. Bozek, I.H. Suzuki, J. Phys. B 28 (1995) 3505.
[7] I.H. Suzuki, N. Saito, J.D. Bozek, Int. J. Mass Spectrom. Ion Processes 136 (1994) 55.
[8] I.H. Suzuki, N. Saito, Int. J. Mass Spectrom. Ion Processes 163 (1997) 229.
[9] W. Eberhardt, T.K. Sham, R. Carr, S. Krummacher, M. Strongin, S. Weng, D. Wesner, Phys. Rev. Lett. 50 (1983) 1038.
[10] M.C. Nelson, J. Murakami, S.L. Anderson, D.M. Hanson, J. Chem. Phys. 86 (1987) 4442.
[11] I.H. Suzuki, N. Saito, Chem. Phys. 253 (2000) 351.
[12] J.H.D. Eland, Laser Chem. 11 (1991) 259.
[13] M. Simon, M. Lavollee, P. Morin, I. Nenner, J. Phys. Chem. 99 (1995) 1733.
[14] M. Simon, P. Morin, P. Lablanqui, M. Lavollee, K. Ueda, N. Kosugi, Chem. Phys. Lett. 238 (1995) 42.
[15] U. Boesl, J. Grotemeyer, K. Müller-Dethlefs, H.J. Neusser, H.L. Selzle, E.W. Schlag, Int. J. Mass Spectrom. Ion Processes 118 (1992) 191.
[16] F.H. Dorman, J. Chem. Phys. 42 (1965) 65.
[17] W.H. Trott, N.C. Blais, E.A. Walters, J. Chem. Phys. 69 (1978) 3150.
[18] I. Powis, C.J. Danby, Int. J. Mass Spectrom. Ion Phys. 32 (1979) 27.
[19] K. Kimura, S. Katsumata, Y. Achiba, T. Yamazaki, S. Iwata, Handbook of HeI Photoelectron Spectra of Fundamental Organic Molecules, Japan Scientific Societies Press, Tokyo, 1981.
[20] C.R. Brundle, D.W. Turner, M.B. Robin, H. Basch, Chem. Phys. Lett. 3 (1969) 292.
[21] A.P. Hitchcock, C.E. Brion, J. Electron Spectrosc. Relat. Phenom. 19 (1980) 231.
[22] T.K. Sham, B.X. Yang, J. Kirz, J.S. Tse, Phys. Rev. A 40 (1989) 652.
[23] N. Saito, I.H. Suzuki, J. Phys. B 20 (1987) L785.
[24] N. Saito, I.H. Suzuki, Phys. Scr. 49 (1994) 80.
[25] W. Eberhardt, J.E. Rubensson, K.J. Randall, J. Feldhaus, A.L.D. Kilcoyne, A.M. Bradshaw, Z. Xu, P.D. Johnson, Y. Ma, Phys. Scr. T41 (1992) 143.
[26] I.H. Suzuki, N. Saito, J. Chem. Phys. 91 (1989) 5324.
[27] N. Saito, I.H. Suzuki, J. Chem. Phys. 91 (1989) 5329.